Clays and Clay Minerals, Vol. 69, No. 4:399–405, 2021

A MOLECULAR DYNAMICS SIMULATION STUDY OF Fe-CONTAINING PALYGORSKITE

Zhijun Lu, Jinhong Zhou*, and Xiancai Lu

[1]State Key Laboratory for Mineral Deposits Research, School of Earth Sciences and Engineering, Nanjing University, Nanjing, Jiangsu 210023, People's Republic of China

Abstract—Fe is a common substituent in palygorskites (Plg), but its effect on the microscopic properties is unclear. In the current study, molecular dynamics (MD) simulations were carried out to investigate the effect of Fe on the properties of the nano-pores in Plg. The structures and dynamics of water and Na^+ ions in the pores were computed by analyzing the MD trajectories. The results revealed that for both Fe-containing and ordinary Plg, zeolitic water molecules can diffuse into the pores with very low mobility whereas Mg-coordinated water fails to escape. Na^+ ions show no obvious diffusivity because they are fixed above the Si–Osix-membered rings. Detailed comparison indicates that Fe-substitution has no significant influence on the pore properties of Plg.

Keywords—Fibrous clay mineral · Iron · Molecular dynamics simulation · Palygorskite

INTRODUCTION

Palygorskite (Plg) is a fibrous clay mineral (Galán, 1996). Due to its significant porosity and specific surface area, Plg has been used widely in industry and engineering and, therefore, is a very important non-metallic mineral (Singer & Galán, 2000). In practical applications, Plg is used as an adsorbent to treat toxic metal ions, organic contaminants, etc., and also as a molecular sieve to separate oil and water (Shariatmadari et al., 1999; Frost et al., 2010; Chen et al., 2011; Sheikhhosseini et al., 2014; Rusmin et al., 2016; Liu et al., 2018; Zhu et al., 2018). These applications are all based on the unique nano-sized pore structures and interfacial properties of Plg. The physical and chemical properties of the pores are of the utmost importance, therefore.

Palygorskite is an aluminosilicate with Fe as the most common isomorphic substitution (Singer et al., 2011). The Plg reserve in the Jiangsu-Anhui region is the largest in China (Gao et al., 2009) and several studies have reported that Fe is a common feature of the Plg from this area (Yi et al., 1995; Long et al., 1997; Yang & Chen, 2004). Fe substitution usually happens in the octahedral sheets according to Liu et al. (2013). The influence of Fe substitution on the properties of Plg pores has not been investigated previously, however.

The pores of Plg are typically nanosized. Current experimental techniques to quantify directly the pore properties are still difficult and very few studies have been reported. Extended X-ray absorption fine structure (EXAFS) has been applied to study the location of zeolitic water in the crystal tunnels and the dehydration of Plg (Post & Heaney, 2008). To the current authors' knowledge, systematic research on the microstructure and mobility of cations and water molecules in the tunnels of Plg is lacking.

With the development of computational simulations, attempts have been made to develop a reliable forcefield for various clay minerals (Teppen et al., 1997; Titiloye & Skipper, 2001; Cygan et al., 2004). *ClayFF* (Cygan et al., 2004) is the most widely used clay force field. The molecular dynamics (MD) method has been applied widely in the fields of mineral science and geochemistry for decades (Mulla et al., 1984; Skipper et al., 1991; Chang et al., 1995; Liu & Lu, 2006; Wang et al., 2006; Zhang & Choi, 2006; Kumar et al., 2007; Anderson et al., 2010; Greathouse et al., 2016; Giri et al., 2018). The interface properties of smectites have been investigated extensively by using MD simulations (Ferrage et al., 2007, 2010; Liu et al., 2008; Greathouse et al., 2015). In contrast, only a few MD studies were concerned with fibrous clay minerals. Fois et al. (2003) tried to introduce molecular dynamics simulations to explain the stability of a palygorskite-indigo complex (Maya blue paint). The structure of water molecules in the pores of sepiolite and palygorskite was studied by Ockwig et al. (2009) but those authors did not study the spatial distribution and mobility of water molecules. By using MD simulation, Zhou et al. (2016) investigated the distributions and dynamics of zeolitic water in sepiolite pores and found that their mobility is very low due to the nano-confinement effects.

In order to reveal the effect of Fe substitution on the distribution and mobility of water and cations, which is difficult to do experimentally, systematic MD simulations were performed to investigate the microscopic properties of the pores of Fe-containing and Fe-free Plg. Through detailed comparisons between Fe-containing and Fe-free Plg, the influence of Fe substitution could be determined.

METHODS

Models

The initial structures of Fe-containing and Fe-free palygorskites (denoted as Fe-Plg and Al-Plg, respectively) are shown in Fig. 1. Their chemical formulae are $Na_{0.5}(Si_{7.5}Al_{0.5})(Mg_2Al_2)O_{20}(OH)_2(OH_2)_4{\cdot}n(H_2O)$ and

This paper is based on a presentation made during the 4th Asian Clay Conference, Thailand, June 2020.

* E-mail address of corresponding author: zjh12387@126.com
DOI: 10.1007/s42860-021-00144-7

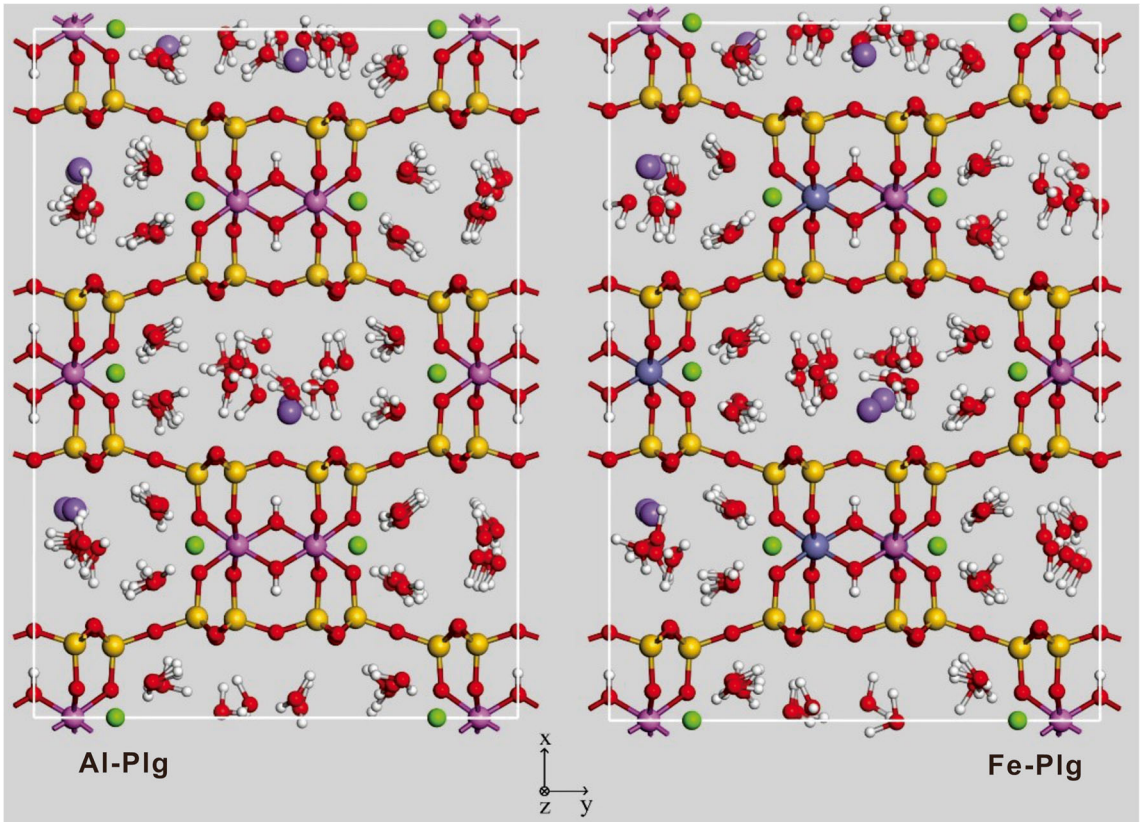

Fig. 1 Snapshots of Plg models. Red = O, Yellow = Si, Green = Mg, White = H, Purple = Na, Cyan = Al, Dark gray = Fe

$Na_{0.5}(Si_{7.5}Al_{0.5})(Mg_2FeAl)O_{20}(OH)_2(OH_2)_4{\cdot}n(H_2O)$. Here OH meant hydroxyl, OH_2 was the coordinated water of Mg, H_2O stood for zeolitic water, and n was taken as 3.5 in this study. The lattice parameters were: $a = 13.286$ Å, $b = 17.848$ Å, $c = 5.242$ Å, $\alpha = 90°$, $\beta = 107.56°$, $\gamma = 90°$. These parameters were taken from the results for Plg samples from Anhui, China (YF Cai). The atomic coordinates of the Plg unit cell were modified from Post and Heaney (2008). The simulation supercells consisted of 8 unit cells ($2a \times 1b \times 4c$) with 3D periodic boundary conditions.

Computation Details

The force field used for the MD simulation was *ClayFF*(Cygan et al., 2004) (details in Table 1). This force field has been applied successfully in simulating clay minerals including smectites, kaolinite, sepiolite, and palygorskite (Cygan et al., 2009; Ockwig et al., 2009; Anderson et al., 2010; Underwood et al., 2016).

ClayFF is a non-bonded forcefield for clay framework. The bond stretch term is required only by the hydroxyl groups.

Table 1 Non-bonded parameters of *Clayff*

Species	Symbol	Charge (e)	ε (kcal/mol)	σ (Å)
Water hydrogen	h*	0.4100	–	–
Hydroxyl hydrogen	ho	0.4250	–	–
Water oxygen	o*	–0.8200	0.1554	3.1655
Hydroxyl oxygen	oh	–0.9500	0.1554	3.1655
Bridging oxygen	ob	–1.0500	0.1554	3.1655
Bridging oxygen with tetrahedral substitution	obts	–1.1688	0.1554	3.1655
Tetrahedral silicon	st	2.1000	1.8405×10^{-6}	3.3020
Tetrahedral aluminum	at	1.5750	1.8405×10^{-6}	3.3020
Octahedral magnesium	mgo	1.3600	9.0298×10^{-7}	5.2643
Octahedral iron	feo	1.575	9.039×10^{-7}	4.9058
Aqueous sodium ion	Na	1.0	0.1301	2.3500

https://doi.org/10.1007/s42860-021-00144-7 Published online by Cambridge University Press

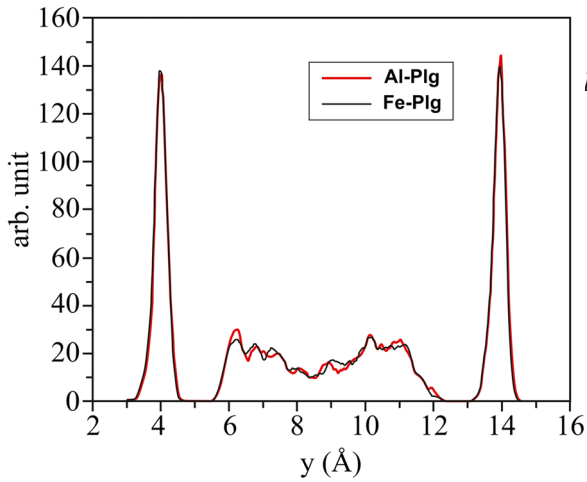

Fig. 2 Density distributions of water O in Plg along the *y* direction

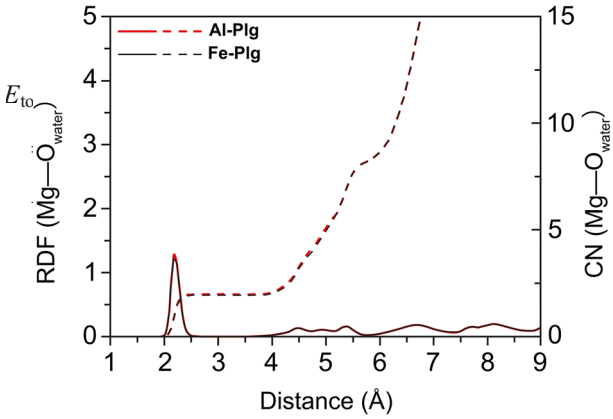

Fig. 4 Radial distribution functions (RDFs) and coordination numbers (CNs) for water O around Mg in the tunnels of Al-Plg and Fe-Plg

Non-bonded van der Waals interactions are calculated through the Lennard-Jones 12-6 potential term:

$$E_{\mathrm{VDW}} = 4\varepsilon_{ij}\left[\left(\frac{\sigma_{ij}}{r}\right)^{12} - \left(\frac{\sigma_{ij}}{r}\right)^{6}\right] \quad (2)$$

where ε and σ represent the van der Waals depth and length, respectively. $\varepsilon_{ij} = \sqrt{\varepsilon_i \varepsilon_j}$ and $\sigma_{ij} = 0.5(\sigma_i + \sigma_j)$. The elec-

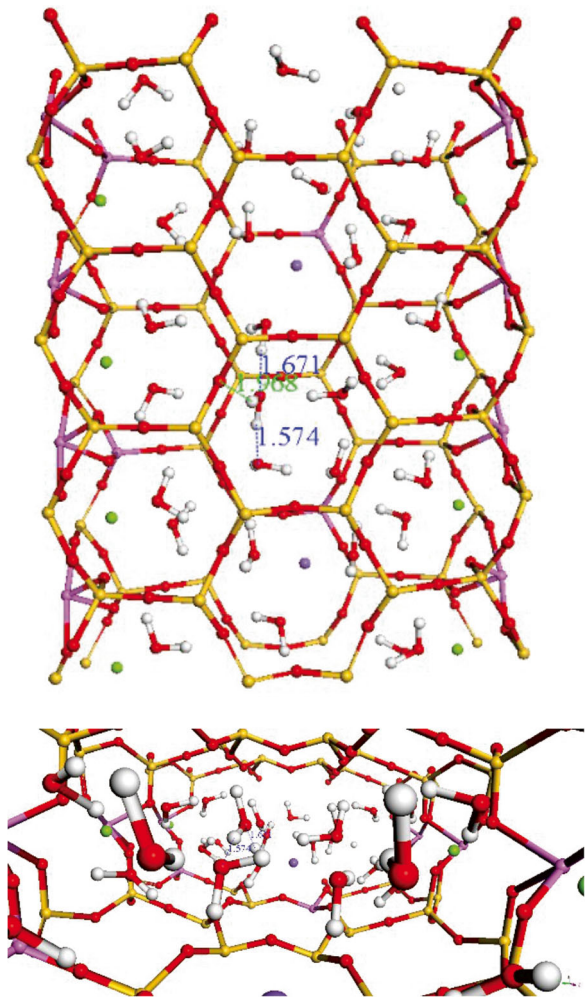

Fig. 3 Structures in the Al-Plg tunnel. Upper: top view; lower: side view parallel to the tunnel. The water–waterH-bonds are shown with blue dashed lines and water–surface oxygen H-bonds are shown with a green dashed line. For clarity, the remainder of the models were removed

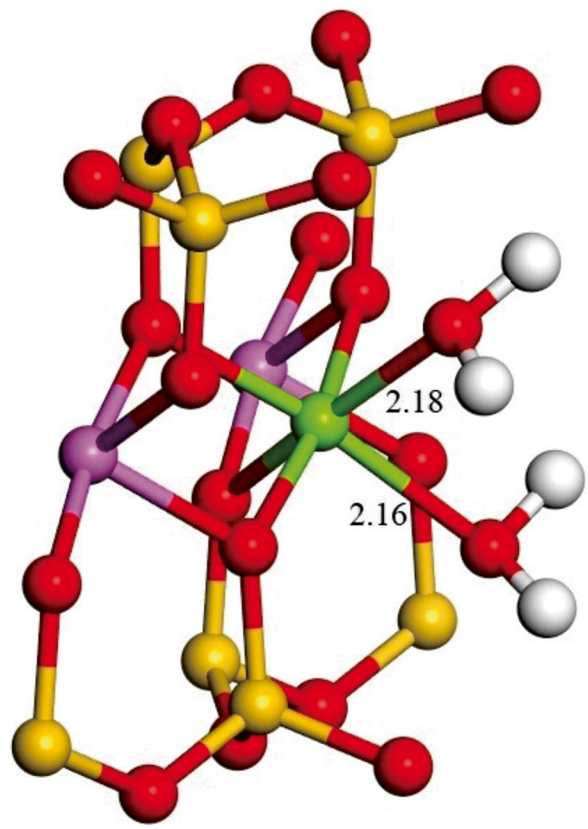

Fig. 5 The coordinated water of edge-Mg derived from the simulation of Al-Plg. Red = O, Yellow = Si, Green = Mg, White = H, Purple = Na, Cyan = Al, Dark gray = Fe

https://doi.org/10.1007/s42860-021-00144-7 Published online by Cambridge University Press

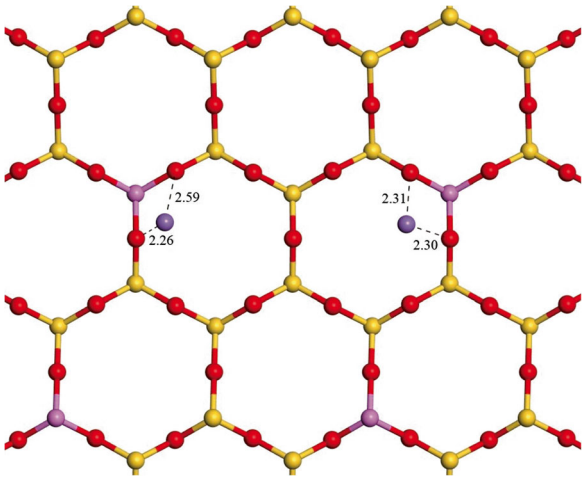

Fig. 6 Snapshot of Na^+ ions on the inner surface of Al-Plg

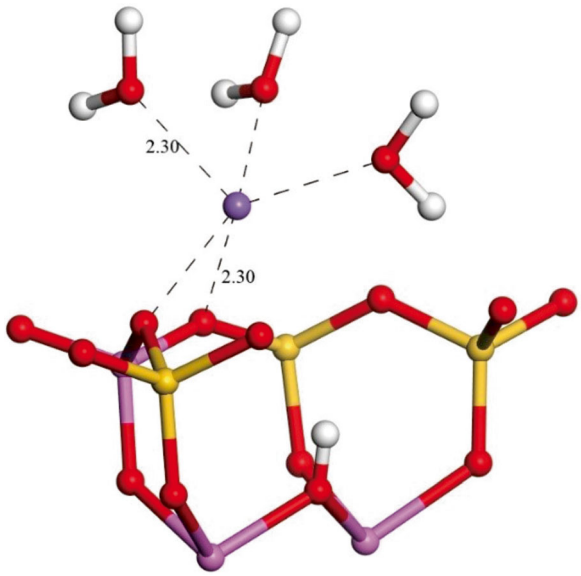

Fig. 7 Snapshot of the coordination structure of Na^+ ions in the pores of Al-Plg

trostatic interactions are calculated through coulombic potential terms and treated using the Ewald summation.

$$E_{\text{coul}} = \frac{q_i q_j}{4\pi\varepsilon_0 r} \tag{3}$$

where q_i and q_j are the partial charge of atom i and j. e is the charge of the electron,

NVT MD simulations were carried out using the *LAMMPS* package (Plimpton, 1995). Each simulation was run for 5 ns with a time step of 1 fs, and the last 3 ns was taken as the production run.

RESULTS AND DISCUSSIONS

Distributions of Water in Pores

The two profiles of the density distributions of water O in Plg pores along the y direction (i.e. parallel to the tunnels) are very similar (Fig. 2). The snapshot for Al-Plg (Fig. 3) was used as an example because the structures in Fe-Plg and Al-Plg were almost the same. By integrating the density distributions and the snapshots it was clear that the sharp peaks on the density distributions denoted the coordinated water of Mg and the shoulders in the middle were zeolitic water.

In the simulation periods of the two Plg models, all coordinated water molecules of Mg atoms vibrated only near the equilibrium positions but could not escape. The radial distribution function (RDF) (Fig. 4) for water molecules around Mg presented a very sharp peak at ~2.18 Å, and its corresponding coordination number (CN) was 2. This peak denoted the coordinated water.

Taking Al-Plg as an example, Fig. 5 showed a snapshot of Mg coordinated water in the pores. Two coordinated water molecules for each Mg and the 4 O atoms in the crystal structure together formed the six-fold coordination of Mg. The agreement between the simulation results of Fe-Plg and Al-Plg indicated that the presence of Fe in the crystal lattice did not affect the local coordination structure of the edge Mg atoms.

On the density distributions (Fig. 2), zeolitic water molecules did not show obvious peaks, indicating that they did not

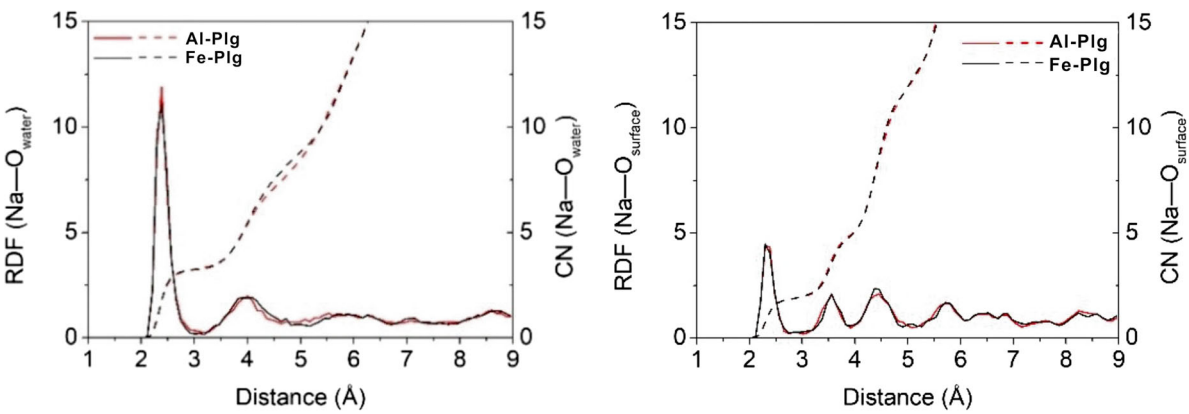

Fig. 8 Radial distribution functions (RDFs) and coordination numbers (CNs) for water O around Na (left panel) and surface O around Na (right panel) in the pores of Al-Plg and Fe-Plg

https://doi.org/10.1007/s42860-021-00144-7 Published online by Cambridge University Press

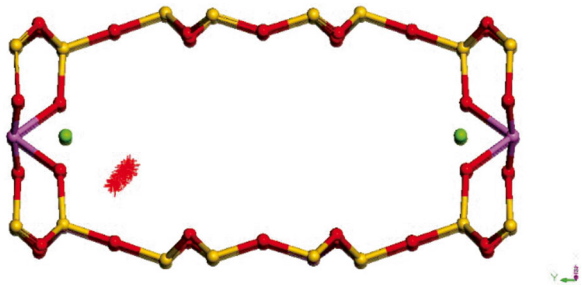

Fig. 9 The trajectory of one Mg-coordinated water in Al-Plg

have specific distributions, but could diffuse freely. H-bonds (Fig. 3) between zeolitic water and six-membered ring oxygen and between the upper zeolitic water and lower zeolitic water could be found clearly. From the comparison of two density distribution curves of Fe-Plg and Al-Plg (Fig. 2), Fe in the structure did not influence the spatial distribution of zeolitic water. The parameters feo and mgo (Table 1) were similar and the interactions between zeolitic water and octahedral Fe/Al were also similar, therefore. On the other hand, the distributions of zeolitic water were affected mainly by interaction with closer Na^+.

Distribution of Na^+

The distribution of Na^+ ions derived from Al-Plg channels is shown as an example (Fig. 6), and the situation in Fe-Plg was very similar. Na^+ was located above the six-memberedSi–O ring on the surface and close to the substituting ion. Na^+ ions, therefore, interacted directly with surface O atoms and the water molecule O (Fig. 7). According to the RDF-CN curve (Fig. 8), each Na^+ ion was coordinated with three zeolitic water molecules, on average, and with two surface O atoms, but did not interact directly with the coordinated water of Mg (Fig. 9). The distance between Na and bound water is >3 Å. The coordinated water of Mg, therefore, vibrated around Mg only. The two RDF-CN curves almost overlapped. The comparisons revealed that the influence of Fe on the distribution and structure of Na^+ was negligible.

Mobility of Pore Species

The MSD (mean squared displacement) curves of the species in Plg tunnels are noted to be very similar (Fig. 10). The curves of Mg-coordinated water were close to 0 $Å^2$, corresponding to the rather rigid coordination as discussed above. The curves of Na^+ ions were almost horizontal, indicating very limited mobility. Using the two models, the MSDs of zeolitic water were notably greater and showed obvious diffusion within the tunnels. The self-diffusion coefficients (D) of zeolitic water was calculated from the MSD curves (Eq. 4). The sampling frequency of MSD was every 100 fs and the sample time was 2 ns. These comparisons showed that the self-diffusion coefficient of zeolitic water in Fe-Plg was a little greater than that in Al-Plg. The magnitudes of self-diffusion coefficients were both ~10^{-11} m^2/s, however. The Fe-substitution in the structure, therefore, did not affect the mobility of the species significantly.

$$D = \frac{1}{2n}\lim_{t\to\infty}\frac{d\langle l^2\rangle}{dt} \quad (4)$$

The MSD pattern of Na^+ showed a plateau which indicated that the movement of Na^+ was very restricted by the Plg tunnels. Previous studies showed that in the interlayer space of smectites, Na^+ ions favor being hydrated and, thus, have notably greater mobility. Their self-diffusion coefficients obtained by fitting MSD curves were of the order of ~10^{-10} m^2/s. New Na^+ forcefield parameters were used by Ho et al. (2019) in *ClayFF* and those authors found that the mobility of Na^+ increased, but the Na^+ MSDs still showed a plateau with new Na^+ parameters in Plg. On the contrary, K^+ ions had relatively low mobility because they preferred staying above the surface Si–Osix-membered rings and bonded simultaneously with surface oxygen atoms and interlayer water molecules. As shown

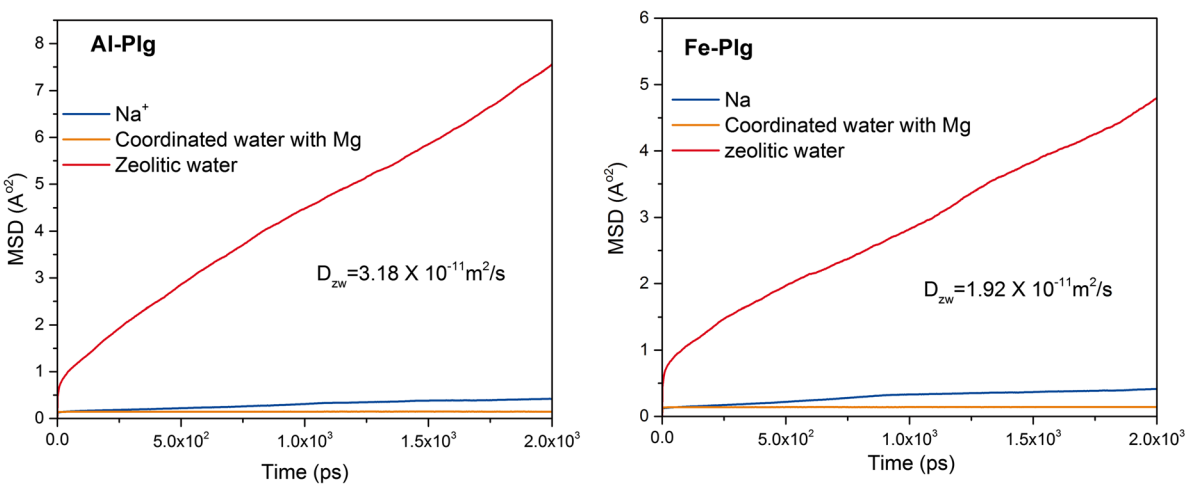

Fig. 10 Mean squared displacement (MSD) curves of species in tunnels of Al-Plg and Fe-Plg

https://doi.org/10.1007/s42860-021-00144-7 Published online by Cambridge University Press

above, Na^+ ions were always fixed above the six-membered rings and, therefore, scarcely showed obvious diffusive behavior. This feature was very similar to that of K^+ ions in smectites. The special distribution of Na^+ was caused by the unique nano-sized tunnels of Plg.

The self-diffusion coefficients of zeolitic water calculated for the two Plg systems were very close, i.e. ~10^{-11} m^2/s. This value was much smaller than that of bulk water (~10^{-9} m^2/s) and also than that of the interlayer water of montmorillonites (~10^{-10}–10^{-9} m^2/s) (Holmboe & Bourg, 2013; Zhang et al., 2014). These values were close to the diffusion coefficient of zeolitic water in sepiolite pores calculated by Zhou et al. (2016). The poor mobility of zeolitic water molecules indicated that the Plg pores had a very strong spatial confining effect on them, which was similar to that of sepiolite.

The mobility results of Na^+ ions and water molecules showed that the one-dimensional nano-sized tunnels of Plg imposed very strong spatial limits on the species. These observations infer that other molecules such as pollutants could also be fixed firmly in the pores.

CONCLUSIONS

In the present study, molecular dynamics simulations were carried out to simulate Fe-containing and Fe-free Plg systems, with the focus on the influence of Fe substitution on the physical and chemical properties of the Plg pores. Through detailed analyses of the MD trajectories, the distribution and mobility of water and cations in the pores were derived. The following conclusions were drawn: (1) Mg-coordinated water vibrated near the equilibrium position and could not diffuse; (2) zeolitic water had much poorer mobility than the bulk and interlayer water in montmorillonites due to the very strong nano-confining effect of the pores; and (3) Na^+ ions were distributed above the Si–Osix-membered rings, and they showed almost no diffusivity. Systematic comparison indicated that the difference between Fe and non-Fe systems was negligible, inferring that the environmentally important properties of Fe-containing Plg, such as adsorption and fixation of toxic substances, were similar to those of ordinary Plg,

ACKNOWLEDGMENTS

The authors acknowledge the National Natural Science Foundation of China (Nos. 42002036 and 41572027) and are grateful to the High-Performance Computing Center (HPCC) of Nanjing University for the numerical calculations (on its blade cluster system) used here.

FUNDING

Funding sources are as stated in the Acknowledgments.

Declarations

Conflict of Interest

The authors declare that they have no conflict of interest.

REFERENCES

Anderson, R., Ratcliffe, I., Greenwell, H. C., Williams, P., Cliffe, S., & Coveney, P. (2010). Clay swelling – a challenge in the oilfield. *Earth-Science Reviews, 98*(3), 201–216.

Chang, F. R. C., Skipper, N. T., & Sposito, G. (1995). Computer-simulation of interlayer molecular-structure in sodium montmorillonite hydrates. *Langmuir, 11*, 2734–2741.

Chen, T., Liu, H., Li, J., Chen, D., Chang, D., Kong, D., & Frost, R. L. (2011). Effect of thermal treatment on adsorption–desorption of ammonia and sulfur dioxide on palygorskite: Change of surface acid–alkali properties. *Chemical Engineering Journal, 166*(3), 1017–1021.

Cygan, R. T., Liang, J.-J., & Kalinichev, A. G. (2004). Molecular models of hydroxide, oxyhydroxide, and clay phases and the development of a general force field. *The Journal of Physical Chemistry B, 108*(4), 1255–1266.

Cygan, R. T., Greathouse, J. A., Heinz, H., & Kalinichev, A. G. (2009). Molecular models and simulations of layered materials. *Journal of Materials Chemistry, 19*(17), 2470–2481.

Ferrage, E., Lanson, B., Sakharov, B. A., Geoffroy, N., Jacquot, E., & Drits, V. A. (2007). Investigation of dioctahedral smectite hydration properties by modeling of X-ray diffraction profiles: Influence of layer charge and charge location. *American Mineralogist, 92*(10), 1731–1743.

Ferrage, E., Lanson, B., Michot, L. J., & Robert, J.-L. (2010). Hydration properties and interlayer organization of water and ions in synthetic Na-smectite with tetrahedral layer charge. Part 1. Results from X-ray diffraction profile modeling. *The Journal of Physical Chemistry C, 114*(10), 4515–4526.

Fois, E., Gamba, A., & Tilocca, A. (2003). On the unusual stability of Maya blue paint: molecular dynamics simulations. *Microporous and Mesoporous Materials, 57*, 263–272.

Frost, R. L., Xi, Y., & He, H. (2010). Synthesis, characterization of palygorskite supported zero-valent iron and its application for methylene blue adsorption. *Journal of Colloid and Interface Science, 341*(1), 153–161.

Galán, E. (1996). Properties and applications of palygorskite-sepiolite clays. *Clay Minerals, 31*(4), 443–453.

Gao, D., Chen, T., Wu, X., Huang, X., & Wang, J. (2009). Rheological properties of aqueous suspensions of palygorskite from Jiangsu and Anhui. *Acta Petrologica et Mineralogica, 28*(6), 665–669.

Giri, A. K., Teixeira, F., & Cordeiro, M. N. D. S. (2018). Structure and kinetics of water in highly confined conditions: A molecular dynamics simulation study. *Journal of Molecular Liquids, 268*, 625–636.

Greathouse, J. A., Hart, D. B., Bowers, G. M., Kirkpatrick, R. J., & Cygan, R. T. (2015). Molecular simulation of structure and diffusion at smectite-water interfaces: Using expanded clay interlayers as model nanopores. *Journal of Physical Chemistry C, 119*(30), 17126–17136.

Greathouse, J. A., Cygan, R. T., Fredrich, J. T., & Jerauld, G. R. (2016). Molecular dynamics simulation of diffusion and electrical conductivity in montmorillonite interlayers. *Journal of Physical Chemistry C, 120*(3), 1640–1649.

Ho, T. A., Criscenti, L. J., & Greathouse, J. A. (2019). Revealing transition states during the hydration of clay minerals. *The Journal of Physical Chemistry Letters, 10*(13), 3704–3709.

Holmboe, M., & Bourg, I. C. (2013). Molecular dynamics simulations of water and sodium diffusion in smectite interlayer nanopores as a function of pore size and temperature. *The Journal of Physical Chemistry C, 118*(2), 1001–1013.

Kumar, P. P., Kalinichev, A. G., & Kirkpatrick, R. J. (2007). Molecular dynamics simulation of the energetics and structure of layered double hydroxides intercalated with carboxylic acids. *Journal of Physical Chemistry C, 111*(36), 13517–13523.

Liu, X.-D., & Lu, X.-C. (2006). A thermodynamic understanding of clay-swelling inhibition by potassium ions. *Angewandte Chemie International Edition, 45*(38), 6300–6303.

https://doi.org/10.1007/s42860-021-00144-7 Published online by Cambridge University Press

Liu, X., Lu, X., Wang, R., & Zhou, H. (2008). Effects of layer-charge distribution on the thermodynamic and microscopic properties of Cs-smectite. *Geochimica et Cosmochimica Acta, 72*(7), 1837–1847.

Liu, H., Chen, T., Chang, D., Chen, D., Qing, C., Xie, J., & Frost, R. L. (2013). The difference of thermal stability between Fe-substituted palygorskite and Al-rich palygorskite. *Journal of Thermal Analysis and Calorimetry, 111*(1), 409–415.

Liu, P., Wei, G., Liang, X., Chen, D., He, H., Chen, T., Xi, Y., Chen, H., Han, D., & Zhu, J. (2018). Synergetic effect of Cu and Mn oxides supported on palygorskite for the catalytic oxidation of formaldehyde: Dispersion, microstructure, and catalytic performance. *Applied Clay Science, 161*, 265–273.

Long, D., McDonald, A., Facheng, Y., Houjei, L., Zili, Z., & Xu, T. (1997). Palygorskite in palaeosols from the Miocene Xiacaowan formation of Jiangsu and Anhui provinces, PR China. *Sedimentary Geology, 112*(3-4), 281–295.

Mulla, D. J., Cushman, J. H., & Low, P. F. (1984). Molecular-dynamics and statistical-mechanics of water near an uncharged silicate surface. *Water Resources Research, 20*, 619–628.

Ockwig, N. W., Greathouse, J. A., Durkin, J. S., Cygan, R. T., Daemen, L. L., & Nenoff, T. M. (2009). Nanoconfined water in magnesium-rich 2:1 phyllosilicates. *Journal of the American Chemical Society, 131*(23), 8155–8162.

Plimpton, S. (1995). Fast parallel algorithms for short-range molecular dynamics. *Journal of Computational Physics, 117*(1), 1–19.

Post, J. E., & Heaney, P. J. (2008). Synchrotron powder X-ray diffraction study of the structure and dehydration behavior of palygorskite. *American Mineralogist, 93*(4), 667–675.

Rusmin, R., Sarkar, B., Biswas, B., Churchman, J., Liu, Y., & Naidu, R. (2016). Structural, electrokinetic and surface properties of activated palygorskite for environmental application. *Applied Clay Science, 134*, 95–102.

Shariatmadari, H., Mermut, A. R., & Benke, M. B. (1999). Sorption of selected cationic and neutral organic molecules on palygorskite and sepiolite. *Clays and Clay Minerals, 47*(1), 44–53.

Sheikhhosseini, A., Shirvani, M., Shariatmadari, H., Zvomuya, F., & Najafic, B. (2014). Kinetics and thermodynamics of nickel sorption to calcium-palygorskite and calcium-sepiolite: A batch study. *Geoderma, 217*, 111–117.

Singer, A. & Galán, E. (2000). *Palygorskite-sepiolite: Occurrences, Genesis and Uses*. Elsevier, Amsterdam.

Singer, A., Huertos, E. G., & Galán, E. (2011). *Developments in Palygorskite-Sepiolite Research: A New Outlook on these Nanomaterials*. Elsevier, Amsterdam.

Skipper, N. T., Refson, K., & McConnell, J. D. C. (1991). Computer-simulation of interlayer water in 2-1 clays. *Journal of Chemical Physics, 94*, 7434–7445.

Teppen, B. J., Rasmussen, K., Bertsch, P. M., Miller, D. M., & Schäfer, L. (1997). Molecular dynamics modeling of clay minerals. 1. Gibbsite, kaolinite, pyrophyllite, and beidellite. *The Journal of Physical Chemistry B, 101*(9), 1579–1587.

Titiloye, J. O., & Skipper, N. T. (2001). Molecular dynamics simulation of methane in sodium montmorillonite clay hydrates at elevated pressures and temperatures. *Molecular Physics, 99*(10), 899–906.

Underwood, T., Erastova, V., & Greenwell, H. C. (2016). Wetting effects and molecular adsorption at hydrated kaolinite clay mineral surfaces. *The Journal of Physical Chemistry C, 120*(21), 11433–11449.

Wang, J., Kalinichev, A. G., & Kirkpatrick, R. J. (2006). Effects of substrate structure and composition on the structure, dynamics, and energetics of water at mineral surfaces: A molecular dynamics modeling study. *Geochimica et Cosmochimica Acta, 70*(3), 562–582.

Yang, J., & Chen, J. (2004). Mineralogical characteristics of palygorskite from Xuyi, Jiangsu. *Volcanology & Mineral Resources, 25*(3), 190–196.

Yi, F. C., Li, H. J., Tian, X., & Zheng, Z. L. (1995). Mineralogy of palygorskite from the Jiangsu-Anhui border area. *Acta Petrologica et Mineralogica, 14*(3), 262–270.

Zhang, J., & Choi, S. K. (2006). Molecular dynamics simulation of methane in potassium montmorillonite clay hydrates. *Journal of Physics B – Atomic Molecular and Optical Physics, 39*(18), 3839–3848.

Zhang, L., Lu, X., Liu, X., Zhou, J., & Zhou, H. (2014). Hydration and mobility of interlayer ions of (Na_x, Ca_y)-montmorillonite: A molecular dynamics study. *Journal of Physical Chemistry C, 118*(51), 29811–29821.

Zhou, J., Lu, X., & Boek, E. S. (2016). Confined water in tunnel nanopores of sepiolite: Insights from molecular simulations. *American Mineralogist, 101*(3), 713–718.

Zhu, J., Zhang, P., Wang, Y., Wen, K., Su, X., Zhu, R., He, H., & Xi, Y. (2018). Effect of acid activation of palygorskite on their toluene adsorption behaviors. *Applied Clay Science, 159*, 60–67.

(Received 23 November 2020; revised 22 June 2021; AE: Jianxi Zhu)